Journal of Materials and Environmental Sciences
ISSN : 2028-2508
CODEN : JMESCN

J. Mater. Environ. Sci., 2018, Volume 9, Issue 2, Page 689-700

https://doi.org/10.26872/jmes.2018.9.2.76

http://www.jmaterenvironsci.com/

Quantum chemical studies and Adsorption Characteristic of 4-hydroxy-3-[1-(2-phenylhydrazinylidene) ethyl] 2H-1-benzopyran-2-one on Mild Steel in Hydrochloric Acid

H. El Attari[1*], S. Mengouch[1], M. Siniti[2], E. Zahidi[2], L. Khamliche[3], A. Kheribech[4]

1.Chemistry Department, Laboratoire de Chimie de Coordination et d'Analytique, Faculty of Science, 24000 El Jadida, University of Chouaib Doukkali, Morocco.

2.Chemistry Department, Equipe de Thermodynamique, Surfaces et Catalyse, Faculty of Science, 24000 El Jadida, University of Chouaib Doukkali, Morocco.

3.Chemistry Department, laboratoire de chimie bio-organiques, Faculty of Science, 24000 El Jadida, University of Chouaib Doukkali, Morocco.

4.Chemistry Department, laboratoire de l'Eau et de l'Environnement, Faculty of Science, 24000 El Jadida, University of Chouaib Doukkali, Morocco.

Received 19 Jan 2017,
Revised 28 Mar 2017,
Accepted 01 Apr 2017

Keywords

- ✓ 4-hydroxy-3-[1-(2 phenylhydrazinylidene)ethyl] 2H-1benzopyran-2-one
- ✓ carbon steel;
- ✓ adsorption;
- ✓ corrosion inhibition;
- ✓ electrochemical measurements.

H. El attari
hassanelattari@yahoo.fr
+212523343003

Abstract

The corrosion of mild steel in hydrochloric acid containing 4-hydroxy-3-[1-(2-phenylhydrazinylidene) ethyl] 2H-1-benzopyran-2-one (HPBO) has been studied at different inhibitor concentrations and temperatures. The effects of the inhibitor have been demonstrated using weight loss and electrochemical measurements. The increase of the inhibitor concentration leads to a decrease in the corrosion rate and in the corrosion current. Inhibition efficiency of 4-hydroxy-3-[1-(2-phenylhydrazinylidene) ethyl] 2H-1-benzopyran-2-one increases with the concentration of inhibitor and decreases with the increase of temperature. The potentiodynamic polarization carried out in 1 M HCl in the absence and presence of the inhibitor clearly proves the fact that this compound behaves as a mixed inhibitor. The adsorption of this compound on the mild steel surface obeys Langmuir's adsorption isotherm. Semi-empirical molecular orbital calculations of HPCO, as molecular model gave useful information to predict the interaction between the surface of metal and the organic molecule as corrosion inhibitor.

1. Introduction

Acid inhibitors find wide application in the industrial field as components in pretreatments, cleaning solutions for industrial equipment, oil-well acidizing, petrochemical processes, and erecting boiler. The highly corrosive nature of aqueous mineral acids on most metals requires some degree of restraint to achieve economic maintenance and operation of equipment. The corrosion of metal and alloys has been the subject of numerous studies due to its importance and its applications in the metallurgical, chemical processing, and oil industries. Its protection against corrosion has attracted much attention [1-6]. Studies of the effect of organic additives on the corrosion rate of mild steel have been the subject of many investigators [7-10]. It has been also found that the molecules contain both nitrogen and Sulphur has exhibited greater corrosion inhibition efficiency in comparison with those contain only one of these atoms [11-14]. Inhibition efficiency I (%) always depends upon the number of active adsorption centers an inhibitor molecule may have, steric factors, aromaticity, the electron density of donor atoms, mode of adsorption, and its capability to form metallic complexes. Corrosion inhibitors have been widely used to decrease hydrogen penetration in steels to reduce the intensity of the corrosive attack of metals exposed to different environments [15-16]. A survey of the available literature reveals that the inhibitive effects of nitriles, aldoximes, ketoximes, azoles derivatives, sulphides, thiazoles, imidazolines, and pyridines have been studied. [17-20]. The efficiency of an organic compound as a successful inhibitor is mainly dependent on its ability to get adsorbed on the metal surface, which consists of the replacement of water molecules at the corroding interface; modifies thus the electrical double layer and forms a protective film that acts a physical barrier blocking the diffusion of ions and the active corrosion sites anodic and/or cathodic [21-26]. It is generally accepted that the first step in the adsorption of an organic inhibitor on a metal surface usually involves the replacement of one or more water molecules adsorbed at the metal surface [27]:

$$nH_2O\ (electrode) + Organic\ (solution) \leftrightarrow Organic\ (electrode) + nH_2O\ (solution)$$

The inhibitor may then combine with inhibitor with freshly generated Fe^{2+} ions on the steel surface, forming metal - inhibitor complex occurs via [28]:

$$Fe \rightarrow Fe^{2+} + 2e^{-}$$
$$Fe^{2+} + Organic\ (electrode) \rightarrow [Fe\text{-}Organic]^{2+}\ (electrode)$$

Recent studies show that a strong coordination bond causes higher inhibition efficiency, the inhibition increasing in the sequence O < N < S < P [29]. Nitrogen and Sulphur containing compounds often provide excellent corrosion protection of mild steel in aggressive environment. The present work was established to study the corrosion inhibition of mild carbon steel in 1 M HCl solution by employing 4-hydroxy-3-[1-(2-phenylhydrazinylidene) ethyl] 2H-1-benzopyran-2-one (HPBO) as a potential corrosion inhibitor of mild steel using three different techniques: weight loss, potentiodynamic polarization and electrochemical impedance spectroscopy. It was found that (HPBO) adsorbs on the steel surface according Langmuir isotherm. Adsorption enthalpy were determined and discussed. Effect of temperature was also investigated and activation parameters were evaluated.

2. Materials and methods:

2.1 Apparatus:

Carbon steel samples with the following composition: 0.38 per cent (C), 0.02 per cent (Si), 0.47 per cent (Mn), 0.01 per cent (P), 0.02 per cent (S) and the remainder iron, were used in the studies .The samples were polished with emery papers from grade 120 to 1200, washed with distilled water, cleaned with acetone, and dried. After being weighed accurately by a balance with high sensitivity, the specimens were immersed in 30 mL 1 M HCl with and without various concentrations of the studied inhibitor at different temperatures. After 6 h of immersion, the specimens were taken out, rinsed thoroughly with distilled water, dried and weighed accurately again. Then the tests were repeated at different temperature immersion time. In order to get good reproducibility, experiments were carried out in duplicate. The corrosion rate (CR) was calculated from the following equation:

$$C_R = \frac{W_1 - W_2}{S.t} \qquad (1)$$

Where W_1 is the initial weight before immersion, W_2 the final weight after the corrosion test, S the geometrical surface area (4 cm^2), and t the period of corrosion test (6 h). The inhibition efficiency I (%) has assessed using a known relation [30]:

$$I(\%) = \frac{CR_0 - CR_{inh}}{CR_0} \times 100 \qquad (2)$$

Where CR_0 and CR_{inh} are the values of corrosion rate without and with inhibitor, respectively.

2.2 *Test Solutions:*

The solution of 1 M hydrochloric acid (Test solution) were prepared for each experiment using analytical grade of hydrochloric acid (37%) and diluted with distilled water from the standard 1 M HCl solution. The concentration range of inhibitor was 2, 5 to 25. 10^{-5} M.

HPBO was prepared according to a laboratory-developed method. In a 100 ml beaker, 1.5 g of 3-acetyl-4-hydroxy coumarin are dissolved in 40 ml of ethanol. The mixture is heated slightly until complete dissolution. Subsequently, the required amount of phenyl hydrazine was added 1.3 times. The yellow precipitate formed is filtered through Buchner and recrystallized from ethanol.

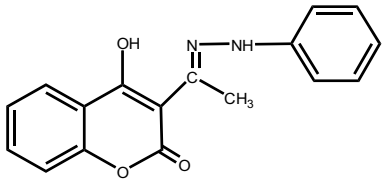

Chemical structure of used inhibitor, 4-hydroxy-3-[1-(2-phenylhydrazinylidene) ethyl] 2H-1-benzopyran-2-one (HPBO)

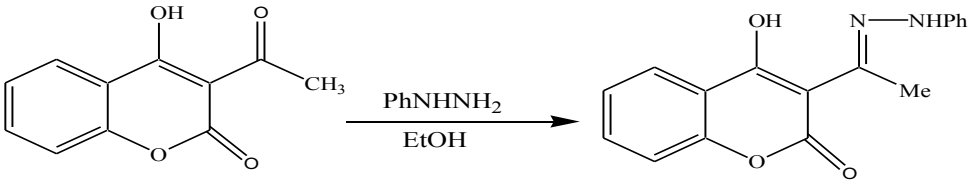

Yield = 51%

Melting point: mp = 236 ° C

δ (ppm)	Multiplicity	Integral	Attribution
2,35	Singulet	3H	Me-C=N-
7-8	Multiplet	9H	Hydrogens of the 2 aromatic rings Hydrogens Of OH and NH
9,75-10,5	Large pic	2H	Hydrogens Of OH and NH

2.3 *Electrochemical measurements:*

The Electrochemical experiments were carried out in the conventional three-electrode cell with a platinum counter electrode (CE) and a saturated calomel electrode (SCE) the working electrode (WE) which was in the form of a square embedded in PVC holder using epoxy resin so that the flat surface was the only surface in the electrode. The working surface area was 1.0 x 1.0 cm², and prepared as described above (Section Weight loss determination). Used materiel is EC-Lab SP 200 Research Grad model potentiostat/galvanostat /FRA. Data were analyzed using an EC-Lab V10.40 software. The polarization curves were recorded by using three-electrode system. The working electrode was first immersed into the test solution for 30 minutes to establish a steady state open circuit potential (E_{ocp}). After measuring the open circuit potential, potentiodynamic polarization curves were obtained with a scan rate of 1 mV/s in the potential range between ±10 V relative to the E_{ocp}. Corrosion current densities values were obtained by extrapolation of the anodic and cathodic Tafel lines to the corrosion potential. Inhibition efficiency I (%) is defined as:

$$I(\%) = \frac{i^0_{corr} - i^{inh}_{corr}}{i^0_{corr}} \times 100 \qquad (3)$$

Where i^0_{corr} and i^{inh}_{corr} represent corrosion current density values without and with inhibitor, respectively.

Electrochemical impedance spectroscopy (EIS) experiments were performed at potential open circuit in the frequency range from 100 kHz to a 10 mHz, with a signal amplitude perturbation of 10 mV. Inhibition efficiency IE (%) is estimated using the following relation:

$$I(\%) = \frac{R^{inh}_{ct} - R^0_{ct}}{R^{inh}_{ct}} \times 100 \qquad (4)$$

Where R^0_{ct} and R^{inh}_{ct} are charge transfer resistance in the absence and presence of the inhibitor, respectively.

3. Results and Discussion

3.1. Electrochemical Measurements:

3.1.1 *Potentiodynamic Polarization:*

Polarization measurements were undertaken to investigate the behavior of mild steel electrodes in 1 M solutions of HCl in the absence and presence of HPBO The current–potential relationship for the mild steel electrode at various test solutions is shown in Figure 1, The effect of various inhibitor concentrations on the corrosion kinetic parameters such as anodic and cathodic Tafel slopes (β_a, β_c), corrosion current density ($i_{corr.}$), corrosion potential (E_{corr}), and inhibition efficiency I (%) obtained from polarization measurements method were recorded and summarized in Table (2).

The values of various electrochemical parameters derived by Tafel polarization of the inhibitor are given in Table 2. Addition of HPBO is seen to affect the partial anodic dissolution of mild steel and also retards the partial cathodic reduction of hydrogen ion, shifts the corrosion potential (E_{corr}) toward more negative (cathodic). Investigation of Table 2 revealed that the values of β_c change slightly in the presence of HPBO where as more pronounced change occurs in the values of β_a, indicating that both anodic and cathodic reactions are effected but the effect on the anodic reactions is more prominent.

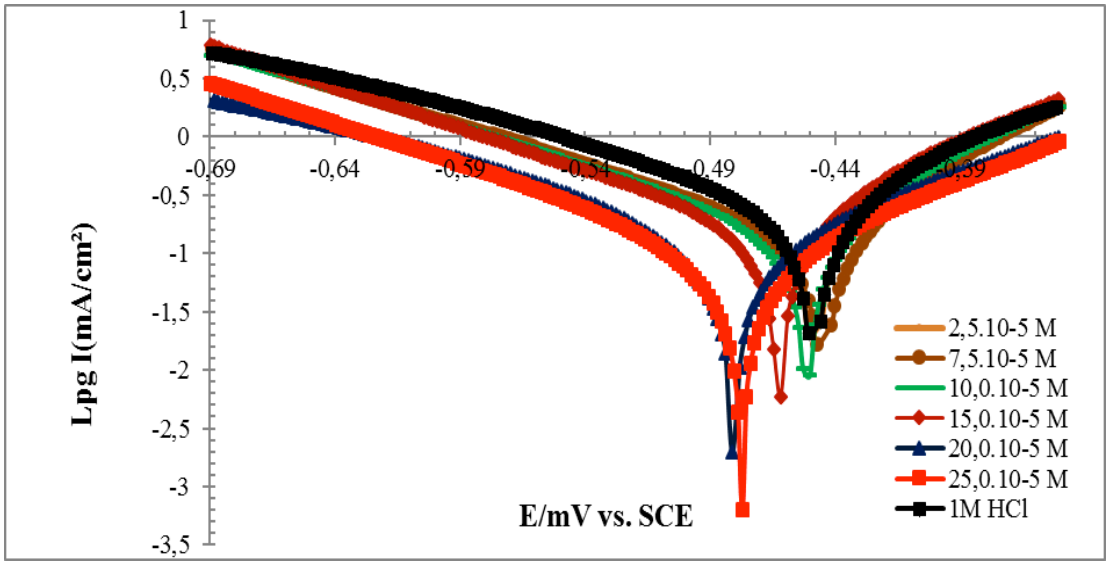

Figure 1: Potentiodynamic polarization curves for carbon steel in 1 M HCl in the absence and presence of different concentrations of HPBO at 298 K measurements

Table 1: Electrochemical parameters of steel samples after immersion in 1M HCl in the absence and presence of HPBO at various concentrations.

C (10^{-5}M)	E_{corr}(mV vs SCE)	I_{corr}(µA cm^{-2})	β_a(mV dec^{-1})	β_c(mV dec^{-1})	*I(%)*
Blank	-407.915	354.369	170.8	174.0	
2.5	-475.732	197.913	140.9	120.8	44.1
7.5	-447.930	143.986	88.0	151.3	59.3
10	-437.738	116.828	73.1	149.8	67.0
15	-435.937	110.368	69.9	140.3	68.8
20	-458.055	68.277	67.9	147.0	80.7
25	-459.858	52.031	64.2	142.1	85.3

Thus, HPBO acted as mixed type, but predominantly anodic inhibitor [31]. The values of corrosion current densities in the absence (i^0_{corr}) and presence of the inhibitor (i^0_{inh}) were used to estimate the inhibition efficiency from polarization. Increase in inhibition efficiencies with increasing concentration of HPBO reveals that inhibition action is due to adsorption on steel surface and the adsorption is known to depend on the chemical structure of the inhibitors.

3.1.2 Electrochemical impedance spectroscopy (EIS):

Nyquist plots for carbon steel in 1 M HCl in the absence and presence of HPBO at various concentrations are shown in Figures 2 and 3. It was concluded from these plots that the impedance response of carbon steel in 1 M HCl had significantly altered after the addition of inhibitors into the test solutions. These diagrams have similar shape throughout all tested concentrations, indicating that almost no change in the corrosion mechanism occurs due to the inhibitor addition [32]. The high frequency loops are not perfect semicircles, which can be attributed to the frequency dispersion as a result of the roughness and inhomogeneous of electrode surface [33]. The semicircles were obtained which cut the real axis at higher and lower frequencies. At higher frequency end, the intercept corresponds to solution resistance (R_s) and at lower frequency end; the intercept corresponds to R_s + R_{ct}. The semicircle radii depend on the inhibitor concentration. The capacitive loop can be attributed to the charge transfer reaction and time constant of the electric double layer and to the surface inhomogeneity of structural or interfacial origin, such as those found in adsorption processes. Furthermore, the diameter of the capacitive loop in the presence of inhibitor is bigger than that in the absence of inhibitor (blank solution) and increases with the inhibitor concentration. This indicated that the impedance of inhibited substrate increased with increasing of the corrosion inhibitor concentration. The values of charge-transfer resistance (R_{ct}) increases while those of the double layer capacitance (C_{dl}) decreases with increasing in HPCO concentration. The inhibitor was determined by the analysis of the equivalent circuit models figures. 3, 4 and 5, and their values for all samples at different HPBO concentrations are shown in Table 3.

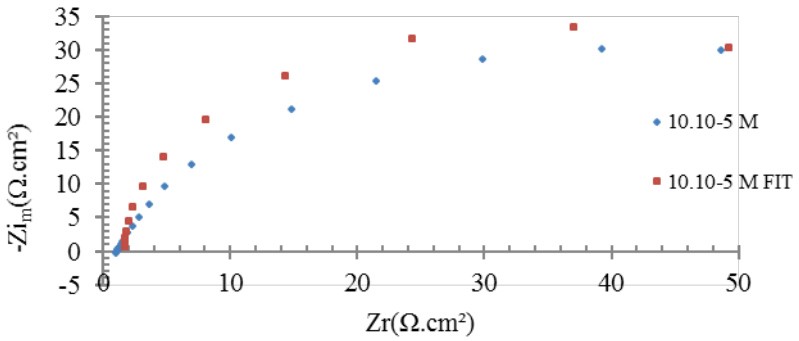

Figure 2: The Nyquist plots for corrosion of carbon steel in 1M HCl and his fit plot at 298 K

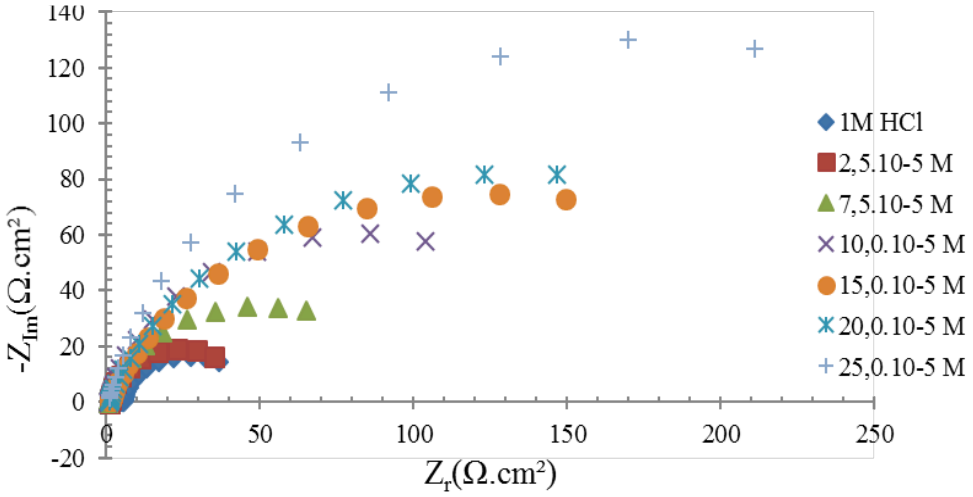

Figure 3: The Nyquist plots for corrosion of carbon steel in 1 M HCl in the absence and presence of different concentrations of HPBO at 298 K.

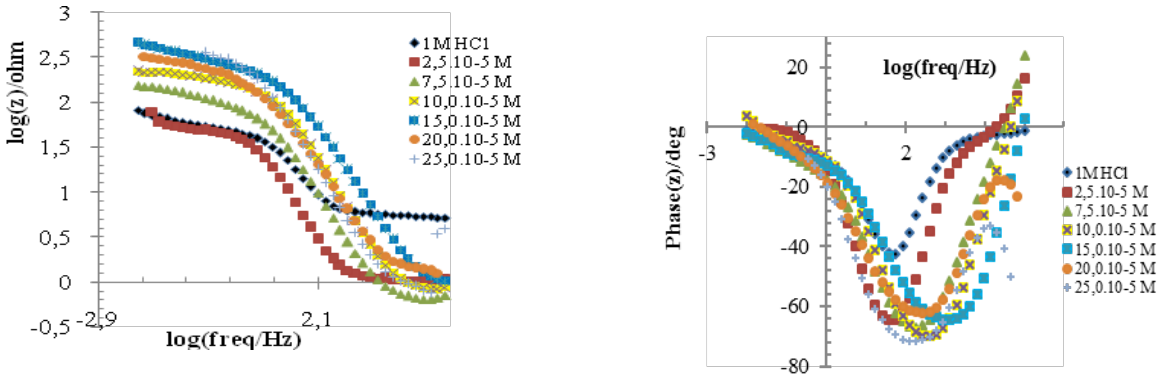

Figures 4-5: Bode plots in the absence and presence of different concentrations of HPCO of mild steel after immersion in the reference solution and with HPBO at 298K.

Inspection of the data in Table I reveals that HPBO appeared to act as an inhibitor over the studied concentration range, R_{ct} values increases, while those of C_{dl} decreases with increasing in HPBO concentration. This is due to increasing the surface. The R_{ct} values indicated that HPBO has a great effect on the dissolution of mid steel in HCl solution. This is due to increasing the surface coverage by the inhibitor which leads to an increase in the inhibition efficiency with increasing inhibitor concentration showing maximum inhibition 87.00 % as shown in Table 3. The capacitance values were calculated using the equation [34]. The impedance function of the CPE is as follows:

$$C_{dl} = (Y_0 \times R_{ct}^{n-1})^{1/n} \quad (5)$$

Where Y_0 is the magnitude of CPE, *R*ct is the charge transfer resistance and *n* is the CPE exponent. Depending on *n*, CPE can represent resistance (Y-1 = R, n = 0), capacitance (Y-1 = C, n = 1), inductance (Y-1 = L, n = -1) and Warburg impedance for n = 0.5 [29]. So, by use of the CPE concept we got excellent fit for the experimental. The impedance data listed in Table 3 indicate that the values of n are found to increase by increasing the inhibitor concentration. This behavior was the result of an increase in the surface coverage by the inhibitor molecules, which led to an increase in the inhibition efficiency.

Table 2: Electrochemical parameters of impedance for carbon steel in 1 M HCl without and with of different concentrations of HPBO at 298 K.

C (10^{-5}M)	R_{ct} (Ω cm^2)	C_{dl} (μF cm$^{-2}10^{-6}$)	Y_0 ($S^nW^{-1}cm^{-2}10^4$)	n	I(%)
Blank	50.66	575	9.53	0.857	
2.5	66.49	556	8.43	0.884	23.80
7.5	113.40	362	7.86	0.792	55.30
10	208.00	314	6.83	0.873	75.60
15	375.10	259	4.22	0.891	86.50
20	380.00	192	3.58	0.862	86.70
25	390.00	180	2.46	0.882	87.00

The decreasing in the capacitance, which can resulted from a decrease in local dielectric constant and/or an increase in the thickness of the electrical double layer, was suggested that the inhibitor molecules acted by adsorption at the metal/solution interface [35]. A decrease in Y_o after the addition of HPBO may be either due to desorption of water molecules from the surface of the electrode followed by adsorption of inhibitor on the surface which results in a decrease in local dielectric constant or an increase in the thickness of the double layer. Further inspection of Table 3 also reveals that n increases with increasing concentration of HPBO. The value increase of n in presence of inhibitor compared to blank represents the decrease in inhomogeneity because of formation of a protective inhibitory film. A similar observation has been reported by several authors [36].

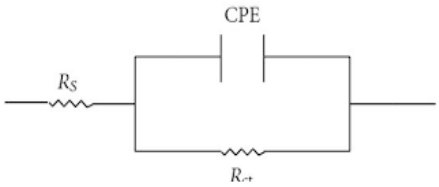

Figure 6: Suggested equivalent circuit model for the studied systems.

3.2. Gravimetric experiment:

Values of inhibition efficiency I (%) and corrosion rate C_R (mg.m^{-2}.s^{-1}), and the surface coverage (θ) obtained from weight loss method for various concentrations of HPBO after 6 h immersion are summarized in Table 4. From the examination of Figures. 7 and 8 and Table 4 and 5, one can see that the addition of HPBO reduces the current density. The reduction is more pronounced with the increase of the inhibitor concentration. Table 5 that the coverage is increased from 0,602 to 0,700. This behavior indicates that the weight loss curves of the mild steel samples with addition of the inhibitor in 1 M HCl at various temperatures are shown in Figure 7. It was observed that HPBO inhibits the corrosion of mild steel in HCl solution, at all concentrations used in study i.e. 2,5-25,0. 10^{-5} M. Weight loss of mild steel decreased with increasing inhibitor concentration. The results showed clearly that corrosion rate decreased significantly with addition of the inhibitor and then decreased gradually with increasing inhibitor concentration, while inhibition efficiency increased with increasing inhibitor concentration. Maximum inhibition efficiency was shown at 25. 10^{-5} M concentration of the inhibitor reached maximum value of 70 % at 298 K. It is evident from the Table 5 that the surface coverage is increased from 0,602 to 0,700. This behavior indicates that the adsorbed molecules formed a barrier film on the mild steel surface [28] and inhibit the corrosion processes via increasing the surface coverage of the electrode surface. The influence of solution temperature on inhibition efficiency showed that inhibition efficiency decreases with

increase in temperature 298K to 308 K. This behavior indicates that the adsorbed molecules formed a barrier film on the mild steel surface [28] and inhibit the corrosion processes via increasing the surface coverage of the electrode surface.

Table 3: Gravimetric measurements parameters for mild steel in 1M HCl containing various concentrations of HPBO at different temperatures.

C (10^{-5}M)	ΔW			C_R		
	298K	303K	308K	298K	303K	308K
Blank	0.120	0.178	0.192	0.0070	0.0111	0.0120
2.5	0.050	0.085	0.109	0.0030	0.0053	0.0068
7.5	0.046	0.082	0.097	0.0028	0.0051	0.0060
10	0.044	0.080	0.093	0.0027	0.0050	0.0058
15	0.040	0.070	0.091	0.0025	0.0044	0.0057
20	0.039	0.060	0.081	0.0024	0.0038	0.0051
25	0.036	0.054	0.079	0.0022	0.0034	0.0049

The influence of solution temperature on inhibition efficiency showed that inhibition efficiency decreases with increase in temperature 298 K to 308 K. The decrease in inhibition efficiency with temperature may be attributed to desorption of the inhibitor. For the inhibition of the carbon-steel corrosion in different media there have been used organic compounds containing Sulphur, oxygen and nitrogen. The results show that most inhibitors act through adsorption on the metal surface. The investigation of HPBO gives good inhibitive performance in hydrochloric acid solutions. The good inhibitive performance in this study may be attributed to the presence of nitrogen as well as oxygen atom and double bonds in the same molecule.

Table 4: Gravimetric measurements parameters for mild steel in 1M HCl containing various concentrations of HPBO at different temperatures.

C (10^{-5}M)	Θ			*I(%)*		
	298K	303K	308K	298K	303K	308K
Blank						
2.5	0.602	0.525	0.432	60.2	52.5	43.2
7.5	0.615	0.539	0.494	62.0	54.0	49.4
10	0.629	0.553	0.519	63.0	55.3	51.9
15	0.661	0.606	0.527	66.1	60.6	52.7
20	0.671	0.661	0.579	67.1	66.1	57.9
25	0.695	0.699	0.591	69.5	70.0	59.1

Organic inhibitors containing heteroatoms such O, N and S are found to have higher basicity and electron density and, thus, act as corrosion inhibitors. The heteroatoms are the active centers for the process of adsorption on the metal surface [37].

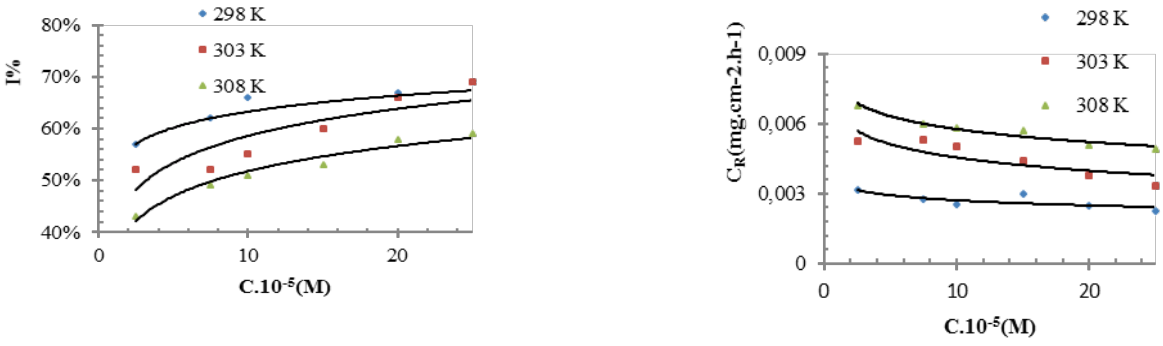

Figures 7-8: Dependence of the percentage inhibition efficiency *I* (%) and corrosion rate on the inhibitor concentration.

3.3. Adsorption isotherm and thermodynamic activation parameters:

The inhibition of metal corrosion by organic compounds is attributed to either the adsorption of inhibitor molecule or the formation of a layer of insoluble complex of the metal on the surface which acts as a barrier between the metal surface and the corrosive medium The protective action of an inhibitor in metal corrosion is often associated with chemical or physical adsorption involving a variation in the charge of the adsorbed substance and transfer of charge from one phase to the other [38- 40]. The coverage of the metal surface by the compound is very useful in discussing the adsorption characteristics. The values of the degree of surface coverage Θ were evaluated at different concentrations of the inhibitor in 1M HCl solution. In our present study the observed data fit the curves lead to Langmuir adsorption isotherm, which is represented by equation:

$$log\ C/\Theta = logC - logK_{ads}$$

Where Θ is the degree of surface coverage, C is the concentration of the inhibitor solution and K_{ads} is the equilibrium constant of adsorption of inhibitor on the metal surface. The above adsorption isotherm reveals that there is no interaction between the adsorbate and adsorbent [41]. Attempts were made to fit Θ values to various adsorption isotherms. A straight-line relationship was obtained when surface coverage Θ was plotted against C/Θ, thereby clearly proving that the adsorption of HPBO on the metal surface from 1M HCl obeys Langmuir adsorption isotherm. The equilibrium constant of adsorption of HPBO on the surface of metal is related to the free energy of adsorption (ΔG_{ads}) which is calculated by the following Equation:

$$K_{ads} = \frac{1}{55,5} \times exp\left(\frac{-\Delta G_{ads}}{RT}\right) \qquad (8)$$

Where, R is the gas constant, T is the temperature and K_{ads} is the equilibrium constant of adsorption. The values of K_{ads} obtained from the intersection of Langmuir's isotherms to the origin were reported in Table 6; the high values of K_{ads} were obtained for the different concentrations tested in diluted hydrochloric acid indicated that the compound is adsorbed on the alloy surface. The physisorption process reflects the type of interaction with Van der Waals forces between the molecules of adsorbed inhibitor and the metal surface with values below -20 ($kJmol^{-1}$). However, for the chemisorption process, the interaction involves sharing charges and coordinate bond formation between the steel surface and the organic molecules with values above -40 ($kJ.mol^{-1}$) [42]. The negative values of ΔG_{ads} almost equal to16, 50 ($kJ.mol^{-1}$) suggested that the adsorption of HPBO on to metal surface is a spontaneous process of physisorption and the adsorbed layer is stable.

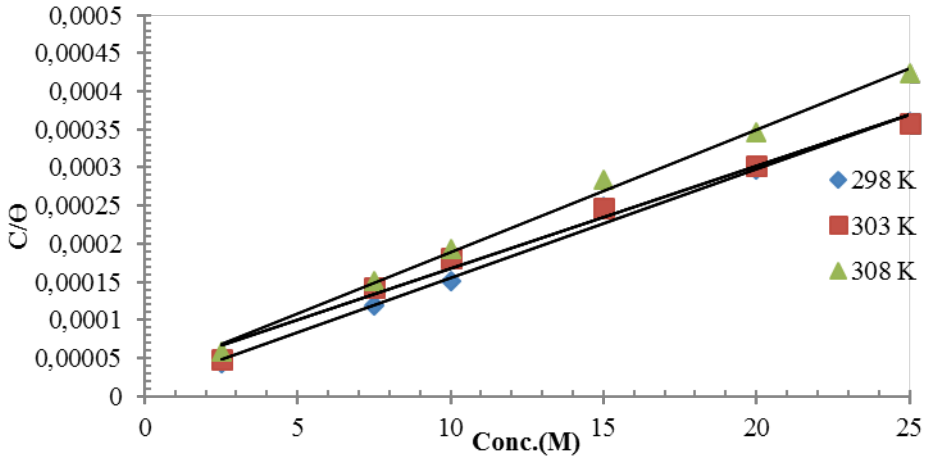

Figure 9: Dependence of C/θ on concentration in the presence of HPBO at 298 K

Table 5: Thermodynamic parameters for studied inhibitor from experimental adsorption isotherm.

T (K)	K_{ads}	ΔG_{ads} ($kJ.\ mol^{-1}$)	ΔH_{ads} ($kJ.\ mol^{-1}$)	ΔS_{ads} ($kJ.mol^{-1}.\ K^{-1}$)	R^2
298	$10.00\ 10^4$	-16.70	36.17	0.065	0.990
303	$33.30\ 10^5$	-15.78	36.17	0.067	0.985
308	$33.30\ 10^5$	-16.04	36.17	0.065	0.995

3.4. Effect of temperature

It has been reported in the literature, that when the temperature increases, the corrosion rate also increases and hence the efficiency of inhibiting organic compounds decreases [43-45]. Therefore, it is also important to evaluate the effect of this variable. In order to study the effect of temperature on the inhibition efficiencies of HPBO, weight loss measurements were carried at three temperature values. The various corrosion parameters obtained are listed in Table 7. The dependence of corrosion rate at temperature can be expressed by Arrhenius equation and transition state equation:

$$C_R = k \exp(\frac{-E_a}{RT}) \qquad (9)$$

$$C_R = \mu' \frac{RT}{Nh} \exp\left(\frac{\Delta S_a}{R}\right) \exp(-\frac{\Delta H_a}{RT}) \qquad (10)$$

where, E_a is apparent activation energy, k is the pre-exponential factor, ΔH_a is the apparent enthalpy of activation, ΔS_a is the apparent entropy of activation, h is Planck's constant and N is the Avogadro number; A linear plot between log (C_R) vs. 1/T, with a slope of ($-\Delta H_a/2.303R$), from which the values of ΔH_a were calculated and listed in Table 7. Inspection of these data reveals that the ΔH_a values for the dissolution reaction of carbon steel in 1M HCl in the presence of HPBO are higher than that in the absence of inhibitors and that the adsorption of inhibitor is an exothermic process [46].The positive signs of ΔH_a reflect that the dissolution of carbon steel is slow in the presence of inhibitor.

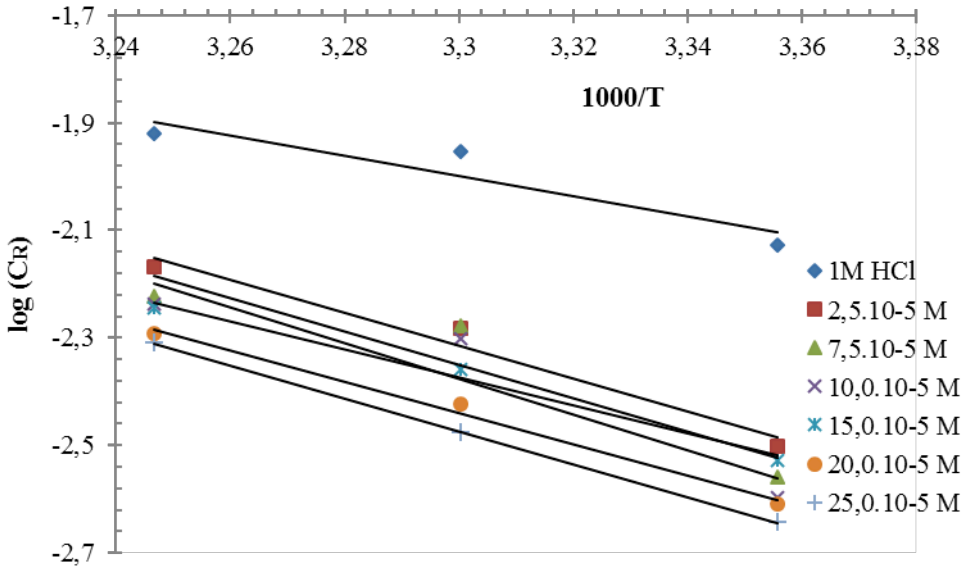

Figures 10: Arrhenius plot for mild steel corrosion in 1M HCl in the absence and presence of HPBO

Table 6: Thermodynamic parameters for studied inhibitor from experimental adsorption isotherm.

C(10^{-5} M)	ΔH_a (kJ.mol^{-1})	ΔS_a (J.mol^{-1}.K^{-1})	k (g.m^{-2}.h^{-1})	E_a (kJ.mol^{-1})	R^2	E_a - ΔH_a
1M HCl	33.80	-186.22	1.89 10^4	36.41	0.872	2.61
2.5	56.16	-156.93	6.33 10^7	58.68	0.971	2.52
7.5	56.96	-156.09	7.98 10^7	59.48	0.875	2.52
10	61.17	-150.27	4.00 10^8	63.69	0.904	2.52
15	47.28	-170.00	1.62 10^6	49.80	0.989	2.52
20	53.29	-162.08	1.51 10^7	55.81	0.992	2.52
25	56.03	-158.44	4.16 10^7	58.55	0.999	2.52

It could be shown from the obtained data the presence of the investigated compound, that thermodynamic activation functions (E_a) of the corrosion in mild steel in 1 M HCl solution in the presence of the inhibitor is higher than those in free acid solution indicating that the inhibitor lowers the inhibition efficiency at higher

temperature, suggesting that the higher energy barrier for the corrosion process in inhibited solution associated with physical adsorption between the investigated compound and the alloy surface [46-49]. The lower values of (E_a) in the absence of inhibitor when compared to in its presence indicates physisorption of the corrosion inhibitor [50]. According to Radovici, cited by Popova et al. [51], the positive signs of ΔH_a reflect the endothermic nature of the mild steel dissolution process. The analysis of results of Table 6 shows that the values of ΔH_a enhance with the inhibitor suggesting that the energy barrier of corrosion reaction increases with presence of HPBO.

3.5 Theoretical parameters predicating:

Among the quantum chemical methods for the assessment of corrosion inhibitors, the functional theory of density, DFT has shown significant promise [52]. Quantum chemical calculations have proved to be a very powerful tool for studying corrosion inhibition mechanism [53]. Quantum chemical calculations were employed to study the effect of the structure on the adsorption of the investigated molecule. To explore the theoretical and experimental consistency, quantum chemical calculations were performed with full geometry optimizations using Gaussian-03 program [54].

Recently, density function theory (DFT) has been used to analyze the characteristics of the inhibitor/surface mechanism and to describe the structural nature of the inhibitor on the corrosion process. Thus, in our present investigation, quantum chemical studies have been successfully implemented to correlate the theoretical calculations of HPBO with his experimental results. Figure 11 shows the optimized geometry of HPBO. Frontier orbital density distribution is useful in predicting adsorption centers of the HPBO molecule responsible for the interaction with metal surface atoms.

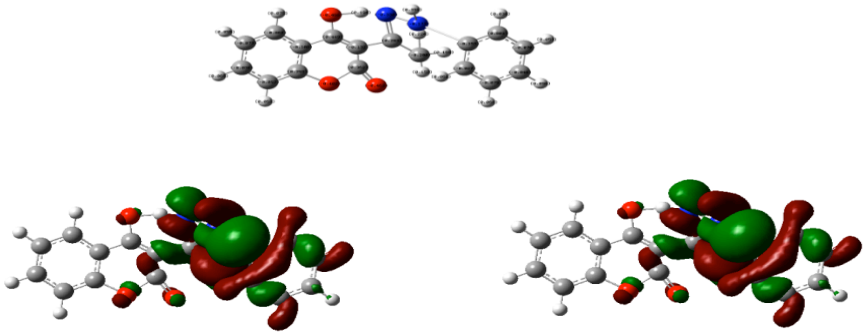

Figures 11-12-13: Optimized structures and Frontier molecular orbital density distributions HOMO (left) and LUMO (right) of HPBO.

Molecular orbital E_{HOMO}, energy of the lowest unoccupied molecular orbital E_{LUMO}, the energy ΔE_{gap} between LUMO and HOMO (E_{LUMO} - E_{HOMO}), and dipole moment (μ) were obtained for the HPBO molecule to predict their activity toward metal surface. High value of E_{HOMO} probably indicates a tendency of the molecule to donate electrons to appropriate acceptor molecules with low energy and empty molecular orbital. E_{LUMO} indicates the ability of the molecule to accept electrons. The lower the value of E_{LUMO}, the more probable is that the molecule would accept electrons. According to frontier orbital theory, the reaction of reactants mainly occurs on L_{HOMO} and L_{LUMO} [55-58]. So, the smaller gap (ΔE) between E_{HOMO} and E_{LUMO} is the more probable to donate and accept electrons. The values of ΔE in Table 8, suggesting the strongest ability of HPBO to form coordinate bonds with d-orbitals of metal through donating and accepting electrons, is in good agreement with the experimental results.

Table 7: Quantum chemical parameters calculated at DFT for HPBO

Inhibitor	Total energy (eV)	E_{HOMO} (eV)	E_{LUMO} (eV)	ΔE_{gap} (eV)	μ (Debye)
HPCO	-568.4586	-6.6643	-4.3016	2.3628	6.2478

Table 8: The calculated quantum chemical parameters of HPBO.

I : Ionisation energie (ev)	5.032
A : Electronic affinity (ev)	4.111
X : Electronegativity (ev)	4.571
ɳ Hardness (ev)	0.460
σ Softness (ev^{-1})	2.173

The values of dipole moment can explain due to non-uniform distributions of positive and negative charges on the various atoms, which could be related to improvement the dipole–dipole interaction of organic molecules and mild steel surface.

Conclusion

HPBO has been found to inhibit corrosion of mild steel in 1 M HCl solution by polarizing both anodic and cathodic reactions, which corresponds with a mixed-control inhibition mechanism. The processes on the interface mild steely 1 M HCl are described by a simple equivalent circuit including charge-transfer resistance (R_{ct}), a parallel double-layer capacitance, C_{dl} which is distributed and modeled by a CPE and an Ohmic resistance, Rs in series with the other elements. The intensity of the corrosive attack clearly decreases with the addition of HPBO to the solution, modifying the metal surface morphology the adsorption model obeys to the Langmuir adsorption isotherm and the ΔH_a^0 values for the dissolution reaction of carbon steel in 1M HCl in the presence of HPBO are higher than that in the absence of inhibitors indicates that the strong interaction between inhibitor molecules and the mild steel surface.

References

1. H.M. Bhajiwala, and R.T. Vashi, *Bull. Electrochem*. 17 (2001) 441.
2. G.N. Mu, X. Li, *Mater. Chem. Phys*. 86 (2004) 59.
3. S. A. Abd El Maksoud., *Corros. Sci*. 44 (2002) 803.
4. A. Y. Musa, A.A. H. Kadhum, A. Mohamad, M.S. Takriff., *Corros. Sci*. 52 (2010) 3331.
5. I. Ahamad, R. Prasad, M. Quraishi., *Corros. Sci*. 52 (2010) 3033.
6. E. Hamed., *Mater. Chem. Phys*. 121 (2010) 70.
7. H. Ma, S. Chen, L. Niu, S. Zhao, S. Li, D. Li., *J. Appl. Electrochem*. 32 (2002) 65.
8. M. Yadav, U. Sharma., *J. Mater. Environ. Sci*. 2 (2011) 407
9. R. Review, A.Wiley., *J. Corrosion and corrosion control: An introduction to corrosion science and engineering*. 4th ed. Canada.
10. I. Ahamad, M. Quraishi., *Corros. Sci*. 52 (2010) 651.
11. H. Ma, S. Chen, L. Niu, S. Zhao, S. Li, D. Li., *J. Appl. Electrochem*. 32 (2002) 65.
12. R. Solmaz, G. Kardas, B. Yazıcı, M. Erbil., *Corros. Eng. Sci. Technol*. 43 (2008) 186.
13. C. Okafor, B. Liu, X. Liu, Y. G. Zheng., *J. Appl. Electrochem*. 39 (2009) 2535.
14. A.Y. Musa, A.A.H. Kadhum, A.B. Mohamad, M.S. Takriff., *Corros. Sci*. 52 (2010) 3331.
15. M. Quraishi, A. Shukla, K. Sudhish., *Mater. Chem. Phys*. 113 (2009) 685.
16. C. Krishnamurthy, K. Narasimha, H. Chander., *Journal of Molecular Liquids*. 211 (2015) 1026.
17. F. Growcock, W. Frenier, P. Andreozzi., *Corros. Sci.* 45 (1989) 1007.
18. I. Lukovits, E. Kalman, G. Palinkas., *Corros. Sci*. 51 (1995) 201.
19. R. Ayers, Jr. C. Hackerman., *J. Electrochem. Soc*. 110 (1963) 507.
20. I. Ahamad, R. Prasad, M., Quraishi., *Corros. Sci*. 52 (2010) 3033.
21. E. Hamed., *Mater. Chem. Phys.* 121 (2010) 70.
22. M. Quraishi, R. Sardar., *Corros. Sci*. 58 (2002) 748.
23. A. Singh, M. Quraishi., *Corros. Sci*. 52 (2010) 1373.
24. M. Quraishi, F. Ansari, *J. Appl. Electrochem*. 33 (2003) 233

25. A. Singh, M. Quraishi., *J. Appl. Electrochem*. 40 (2010) 1293.
26. F. Deflorian, S. Rossi., *Electrochem. Acta*. 51 (2006) 1736.
27. I. Milosev, J. Pavlinac, M. Hodocsek, A. Lesar., *Experimental and theoretical study Journal of the Serbian society*. 78 (2013) 2069.
28. J.O'M, Bockris, D. Drazic, R. Despic., *Electrochim Acta*. 4 (1961) 325.
29. F. Zucchi, G. Trabanelli, G. Gullini., *Electrochim. Metalform.* 3 (1968) 19.
30. O. Yadav, S. Kumar, G. kaur., *J. heterocyclic letters*. 2 (2014) 251.
31. R. Abdel Hameed, H. Al-Shafey, A. Abul Magd., *J. Mater. Environ. Sci*. 3 (2012) 294.
32. L. Larabi, Y. Harek, M. Traisnel, A. Mansri, *J. Appl. Electrochem*. 34 (2004) 833.
33. R. Salim, E. Ech Chihbi, H. Oudda, Y. ELAoufir, F. El-Hajjaji, A. Elaatiaoui, A. Oussaid, B. Hammouti, H. Elmsellem, M. Taleb, *Der Pharma Chemica,* 8(13) (2016) 200-213
34. A. Fouda, K. Shalabi., J. Electrochem. Sci. 9 (2014) 7038.
35. O.S. Doroshkevych, O.V. Shylo, I.A. Saprukina,. L.A. Konstantinova., *World Journal of Condensed Matter. Physics*. 2 (2012) 1.
36. A. Popova, M. Christov, A. Vasilev, T. Deligeorgiev., *Journal of chemical technology and metallurgy*. 49 (2014) 275.
37. H. Zarrok, S. Al-Deyab, A. Zarrouk, R. Salghi, B. Hammouti, H. Oudda, M. Bouachrine, F. Bentiss, *Int.J. Electrochem. Sci*. 7 (2012) 10338.
38. O. Akalezi, K. Enenebaku, E. Oguzie., *J. Mater. Environ. Sci*, 4 (2013) 217.
39. A. Singh, Shukla, K., Ebenso, E., *Int. J. Electrochem. Sci*., 6 (2011) 5689.
40. E. Oguzie., *Portugaliae Electrochim. Acta*. 26 (2008) 303.
41. I. Langmuir., *J. Amer. Chem. Soc.* 39 (1947) 1848.
42. O. Benali, L. Larabi, Y. Harek., *Journal of Saudi Chemical Society*. 14 (2010) 231.
43. A. El bribri, H. El attari, M. Tabyaoui and M. Siniti, *Mor. J. Chem*. 3 (2015) 286.
44. G.S. Popkirov, R.N. Schindler., *Electrochim. Acta*. 40 (1995) 2511.
45. H.B. Rudresh, S.M. Mayanna., *Corros. Sci*. 19 (1979) 361.
46. I. N. Putilova, S. A Balezin, V. P Barannik., *Metall. Corros. Inhibitors Pergamon Press, New York*. 31 (1960).
47. J. Bockris, B. Yang., *J. Elecrochem. Soc*. 138 (1991) 2237.
48. M.S. Al-Otaibi, A. Al-Mayouf., *Arabian Journal of Chemistry*. 7 (2014) 340.
49. C. Selles, O. Benali, B. Tabti, L. Larabi, Y. Harek, *J. Mater. Environ. Sci*. 3 (2012) 206.
50. S. Hosseini, S. Eftekhar, M. Amiri., *Asian Journal of Chemistry*. 19 (2007) 2574.
51. A. Popova., *Corros. Sci*. 49 (2007) 2144.
52. K. Ramya, J. Abraham., *Journal of the Taiwan Institute of Chemical Engineers*. 52 (2015) 127.
53. Y. Karzazi, M.E. Belghiti, F. El-Hajjaji, B. Hammouti, *J. Mater. Environ. Sci*. 7 (2016) 3916-3929
54. M. Lashgari, R. Arshadi, A. Parsafar, Int. *J. Electrochem. Sci*, 6 (2011) 6290.
55. R. Kubba, K. Khathem., *Iraqi Journal of Science*. 57 (2016) 1041.
56. I.B. Obot, N.O Obi-Egbedi., *J. Mater. Environ. Sci*. 2 (2011) 60.
57. A. Zarrouk, H. Zarrok, L. Salghi, F. Bentiss., *J. Mater. Environ. Sci*. 4 (2013) 177.
58. R. Kumar, R. Karthik, S. Chen, *Int. J. Electrochem. Sci*. 11 (2016) 8892.